Journal of Food Process Engineering

Journal of Food Process Engineering ISSN 1745-4530

INFLUENCE OF THE GEOMETRY ASPECT OF JARS ON THE HEAT TRANSFER AND FLOW PATTERN DURING STERILIZATION OF LIQUID FOODS

A.R. LESPINARD[1] and R H. MASCHERONI[1,2,3]

[1]Centro de Investigación y Desarrollo en Criotecnología de Alimentos (CIDCA), CONICET La Plata – UNLP. La Plata, Argentina, 47 y 116 (B1900AJJ)
[2]MODIAL – Depto. Ing. Química – Facultad de Ingeniería, UNLP, La Plata, Argentina

[3]Corresponding author. TEL: +54-221-425-4853; FAX: +54-221-425-4853; EMAIL: rhmasche@ing.unlp.edu.ar

Accepted for Publication August 4, 2010

doi:10.1111/j.1745-4530.2010.00624.x

ABSTRACT

Natural convection heating of liquid food packed in glass jars of different sizes and volumes during sterilization is simulated by solving the governing equations for continuity, momentum and energy conservation, using the finite element method. The effect of the aspect ratio of the container on temperature distribution, flow pattern, position of the slowest heating zone (SHZ) and cooking value were analyzed. The position of the SHZ varied – depending of container volume and aspect ratio – in the range of 49.39–76.83% and 5.81–19.09% of jar radius and height, respectively. Sterilization times were estimated and differences between 135 and 105 s for containers of a same size of 360 or 660 cm^3, respectively, were predicted depending on jar shape. A prediction model was developed that allows to calculate – with a simple procedure – sterilization times as a function of container dimensions.

PRACTICAL APPLICATIONS

It is frequent in low-volume processing plants that work with foods packed in glass jars to change container size and/or shape between successive batches of production, but maintaining the same process schedule. This leads to products with lack of microbial innocuousness (underprocessing) or with low nutritional or sensory quality (overprocessing). In that sense, in this work velocity and temperature profiles, and the location of the "slowest heating zone" were modeled and simulated using the finite element method for liquid foods in glass jars of different volumes and shapes during their thermal treatment. This information allowed estimate sterilization times as well as quality losses during thermal treatment. Finally, a simplified method for the calculation of sterilization times as a function of container size and shape was developed. This method could be very practical for the design of thermal processes in low-volume productions, whose operators usually lack simulation software and personnel trained in process calculations.

INTRODUCTION

Heat sterilization is one of the most common preservation processes for foods; it makes storage life longer and food safer for human consumption, inactivating deleterious enzymes and destroying pathogenic microorganisms. During this process, heat transfer can occur by conduction or by either natural or forced convection according to food structure and characteristics of the heating system. Conductive heating has been the most studied alternative whereas convective heating has been paid little attention. This is due to the inherent complications to solve simultaneously the coupled heat, mass and momentum balances in liquid and semi-liquid materials (Welti Chanes *et al.* 2005). In liquid foods, natural convection is caused by a density gradient within the liquid due to a temperature gradient. For motionless cases, when natural convection occurs, the SHZ moves toward the bottom of the container. The SHZ is defined as the region within a container of product which receives the lowest sterilization treatment during thermal processes (Zechman and Plug 1989). The

SHZ location, heat transfer properties and the sterilization value distribution through the food system are essential for an efficient and safe process design (Pornchaloempong *et al.* 2003a). This zone can be determined by using direct measurements (e.g., thermocouple) or by mathematical modeling. Thermocouple probes can modify the flow in the container, because the temperature evolution is very sensitive to the velocity field. Marra and Romano (2003) observed that the sensor presence, location and size relative to the can dimensions influenced the estimated cold spot temperature evolution and sterility values. Yet, there is no certainty about a probe located in the SHZ. This fact explains the interest in numerical simulations, which can predict the temperature evolution in the whole dominium of the can (Rabiey *et al.* 2007). For this purpose, computational fluid dynamics (CFD) offers a powerful tool for numerical predictions of the transient temperature and velocity profiles in a still retort during natural convection heating of packed liquid foods. There have been several studies on mathematical modeling and numerical simulation of can sterilization processes. Datta and Teixeira (1988) were first to developed numerical predictions of transient temperature and velocity profiles of a can filled with water. Then, simulations of viscous liquid foods in cans were done by Kumar *et al.* (1990) and Kumar and Bhattacharya (1991). Upon introduction of CFD programs and faster computing abilities, simulation studies for natural convection heating have been conducted for different processing conditions. Ghani *et al.* (1999a) carried out transient numerical simulations of natural convective heating process in canned food sterilization and analyzed the SHZ characteristics. Subsequently, Ghani *et al.* (1999b) modeled temperature, flow patterns, bacteria diffusion and thermal deactivation in a can filled with CMC and heated by condensing steam. These authors also studied the combined effect of natural and forced convection heat transfer during sterilization of viscous orange-carrot soup (Ghani *et al.* 2003). More recently, CFD has been used to study the effect of container shape on the efficiency of the sterilization process (Varma and Kannan 2005, 2006). Conical shaped vessels pointing upwards were found to reach the appropriate sterilization temperature the quickest (Varma and Kannan 2006). Full cylindrical geometries performed best when sterilized in a horizontal position (Varma and Kannan 2005). The sterilization of food pouches (Ghani *et al.* 2002) and solid-liquid food mixtures in cans (Rabiey *et al.* 2007; Kiziltas *et al.* 2010) have also been studied using CFD. All of the above numerical studies were carried out for liquid food products packed in metal cans with constant boundary conditions.

On the other side, food processors frequently lack these calculation tools or skilled personnel for its use. Besides, for low production volumes, it is usual the use of glass jars of different dimensions and shapes. To this end, the development of a simple calculation tool, that allows the calculation of sterilization time as a function of container shape and dimension, will be very useful for preserves processors.

In this work, a numerical analysis describes sterilization of high viscosity liquid in cylindrical glass containers of different sizes, placed in upright position and heated with variable external temperature.

The objectives were: (1) to obtain the transient temperature and velocity profiles, the localization of the SHZ and cooking values for different volumes (360 and 660 cm^3) and different height to diameter ratios (*H/D*); and (2) to develop a mathematical model that allows to estimate – in a simple manner – the sterilization times needed to secure microbial innocuousness for each system food-container-processing conditions.

MATERIALS AND METHODS

Details of System and Glass Containers Sizes

A 2D-axisymmetric dominium of simulation was used for cylindrical glass containers of different sizes and ratios *H/D* (Table 1). These containers sizes were selected to include the range of jar sizes being used in the food industry today as well as to enable us to observe effects of *H/D* ratios for constant volumes. An average value of 0.004 m obtained from destructive glass thickness tests was considered as the thickness of the container wall in the model, to assess the possible effect of the glass walls on heating rates.

A pseudoplastic fluid involving 0.85% w/w sodium CMC solution was used as the model system for the simulation. The properties of this system, given in Table 2, are those reported by Ghani *et al.* (1999a). Steffe *et al.* (1986) suggested that this model could be applicable to vegetable purees (tomato, carrot and green beans) or fruit sauces or purees (apple, apricot and banana), which are regularly canned and preserved, usually by heating. For validating the CFD simulations, experiments were also conducted. Commercial CMC was procured from Anedra S.A., Argentina and a 0.85% w/w solution was pre-

TABLE 1. DIMENSIONS AND *H/D* RATIOS OF THE CONTAINERS USED IN THE SIMULATION MODELS

Volume	(660 cm^3)		(360 cm^3)	
Height *H* (cm)	Diameter *D* (cm)	*H/D*	Diameter *D* (cm)	*H/D*
8.0	11.32	0.70	8.57	0.97
10.0	10.16	0.98	7.71	1.38
12.0	9.31	1.28	7.09	1.84
13.7	8.75	1.56	–	–
14.0	8.66	1.61	6.60	2.34
15.1	8.36	1.80	–	–
16.0	8.14	1.96	6.22	2.87
18.0	7.71	2.33	5.90	3.44
20.0	7.35	2.72	5.64	4.05

H/D, height to diameter ratio.

TABLE 2. THERMO-PHYSICAL PROPERTIES USED IN THE SIMULATION MODEL

Material	Properties	Value /expression	Source
CMC (0.85% w/w)	Density, ρ (kg/m^3)	950	Ghani *et al*. (1999a)
	Specific heat, C_p (J/kg/K)	4,100	
	Thermal conductivity, k (W/m/K)	0.70	
	Thermal expansion coefficient, β (K^{-1})	0.0002	
	Viscosity, μ (Pa s)	4.135–6.219 10^{-2} T + 2.596 10^{-4} T^2 (model system) 2.75 – 4.54 10^{-2} T + 2.05 10^{-4} T^2 (experimental system)	
Glass	Thermal diffusivity (m^2/s)	5.97 10^{-6}	Naveh *et al*. (1983)

CMC, carboxy-methyl cellulose.

pared (experimental system). Rheological rotational analyses of CMC solution were performed at 25, 40, 60 and 80C in a Haake ReoStress 600 (Thermo Haake, Karlsruhe, Germany) with a 1 mm gap plate–plate sensor system PP35. Shear stress was determined as a function of shear rate. An acceleration of 4.167/s^2 was used to increase shear rate from 0 to 500/s. The constants of the second-order polynomial model for this solution are also included in Table 2. Other listed properties are taken to be the same for both systems.

Food materials are in general highly non-Newtonian and hence viscosity is a function of shear rate and temperature with a flow behavior index typically less than one. Due to the extremely high viscosity of CMC, which causes liquid velocities to be very low, the shear rate calculated by Kumar and Bhattacharya (1991) was found to be in the order of 0.01/s. Because of the low shear rate viscosity may be assumed to be independent of shear rate, and the fluid would behave as Newtonian fluid. Due to this fact, in our modeling, CMC viscosity was considered to vary only with temperature.

Density variations were considered to be governed by the Boussinesq approximation which assumes that the density variation in the continuity equation can be neglected (incompressibility assumed). The variation of density with temperature is usually expressed as (Adrian 1993):

$$\rho_{ref} g\left[1-\beta\left(T-T_{ref}\right)\right] \tag{1}$$

where β is the thermal expansion coefficient of the liquid, T_{ref} and ρ_{ref} are the temperature and density at the reference condition. For viscous liquids, the viscous forces are high, then the Grashof number is low indicating that the natural convection flow is laminar.

The thermo-physical properties of glass and fluid, used in the model, are given in Table 2.

SIMULATION MODEL

Governing Equations and Numerical Solution Methodology

The commercial software COMSOL Multiphysics (COMSOL 2005), which is based on the finite element method was used to solve the governing transport equations for defined dominiums and associated boundary conditions. The transient calculations were carried out using a backward Euler scheme. Figure 1 shows the shape of the jar and how it was approximated by a cylinder, along with the different domains and interfaces.

For the container (solid phase), the transfer equation was developed in cylindrical coordinates:

$$\rho\, cp\ \frac{\partial \mathrm{T}}{\partial \mathrm{t}} = \frac{1}{r}\frac{\partial}{\partial r}\left(rk\frac{\partial T}{\partial r}\right)+\frac{\partial}{\partial z}\left(k\frac{\partial T}{\partial z}\right) \text{ at } \Omega_1 \tag{2}$$

For the liquid phase (dominium Ω_2), partial differential equations governing natural convection motion in a cylindrical dominium are the Navier-Stokes equations in cylindrical coordinates (Bird *et al*. 1976) as shown below:

$$\text{Equation of continuity: } \frac{1}{r}\frac{\partial}{\partial r}(r\rho v)+\frac{\partial}{\partial z}(\rho u)=0 \tag{3}$$

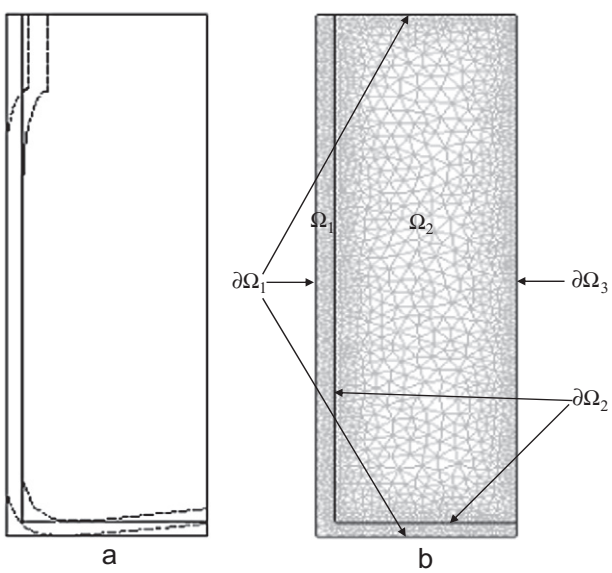

FIG. 1. (A) DIAGRAM OF A GLASS JAR ASSIMILATED TO A CYLINDER AND (B) FINITE ELEMENT MESH SHOWING THE DIFFERENT DOMAINS AND INTERFACES. THE RIGHT-HAND SIDE OF FIGURE IS THE AXIS OF SYMMETRY

Energy balance:

$$\frac{\partial T}{\partial t}+v\frac{\partial T}{\partial r}+u\frac{\partial T}{\partial z}=\frac{k}{\rho c_p}\left[\frac{1}{r}\frac{\partial}{\partial r}\left(r\frac{\partial T}{\partial r}\right)+\frac{\partial^2 T}{\partial z^2}\right] \quad (4)$$

Momentum balance in the vertical direction (z) with the Boussinesq approximation:

$$\rho\left(\frac{\partial u}{\partial t}+v\frac{\partial u}{\partial r}+u\frac{\partial u}{\partial z}\right)=-\frac{\partial p}{\partial z}+\mu\left[\frac{1}{r}\frac{\partial}{\partial r}\left(r\frac{\partial u}{\partial r}\right)+\frac{\partial^2 u}{\partial z^2}\right]+\rho_{ref}g\left[1-\beta\left(T-T_{ref}\right)\right] \quad (5)$$

Momentum balance in the radial direction (r):

$$\rho\left(\frac{\partial v}{\partial t}+v\frac{\partial v}{\partial r}+u\frac{\partial v}{\partial z}\right)=-\frac{\partial p}{\partial r}+\mu\left[\frac{\partial}{\partial r}\left(\frac{1}{r}\frac{\partial}{\partial r}(rv)\right)+\frac{\partial^2 v}{\partial z^2}\right] \quad (6)$$

Interface and Boundary Conditions

At the glass jar boundary: the temperature sensed at jar surface (T_w) was considered as a prescribed value in the simulation model (Eq. 7). This temperature is variable. In the first stage of heating, it increases from its initial value to up to 121C. Later, it remains constant at this value up until the needed sterilization time is reached. This profile is characteristic to low-capacity sterilizers, normally used for thermal processes in low-volume productions.

$$T=T_w(t), \text{ at } \partial\Omega_1 \quad (7)$$

At food boundary, $r=R_{int}$,

$$u=0,\ v=0, \text{ for } z_{wt}\le z\le H. \quad (8)$$

At the bottom of the food, $z=z_{wt}$,

$$u=0,\ v=0, \text{ for } 0\le r\le R_{int}. \quad (9)$$

At the top of the food, $z=H$,

$$u=0,\ v=0, \text{ for } 0\le r\le R_{int}. \quad (10)$$

At the solid–liquid interface the heat flux continuity condition gives:

$$k_s(\nabla T_s\cdot n)=k_l(\nabla T_l\cdot n) \quad (11)$$

Symmetry:

$$\frac{\partial T}{\partial r}=0,\ \frac{\partial u}{\partial r}=0,\ v=0, \quad \text{at } \partial\Omega_3 \quad (12)$$

Initially, the temperature is uniform and the fluid is at rest,

$$T=T_i, \text{ at } \Omega_1 \text{ and } \Omega_2 \quad (13)$$

$$u=0,\ v=0, \text{ at } \Omega_2 \quad (14)$$

Assumptions Used in the Numerical Simulation

To simplify the problem, the following assumptions were made: (1) jars were approximated to the geometry of a cylinder (see Fig. 1a); (2) axial symmetry, which reduces the problem from three-dimensional to two-dimensional; (3) heat generation due to viscous dissipation is negligible due to the use of highly viscous liquid with very low velocities; (4) boussinesq approximation is valid (ρ_{ref} = 1,040 kg/m^3 at T_{ref} = 20C); (5) essential boundary conditions were considered and the effect of surface heat transfer coefficient was neglected; (6) the condition of no-slip on the inner wall of the glass jar is valid; (7) the resistance to heat transfer of metallic lids is negligible; and (8) the thermal properties of the glass jar and fluid are constant.

Mesh and Time Step Details

The boundary layer occurring at the heated walls and its thickness are the most important parameters for the numerical convergence of the solution. Temperature and velocities have their largest variations in this region. To adequately resolve this boundary layer flow, i.e., to keep discretization error low, the mesh should be optimized and a large concentration of grid points is needed in this region. If the boundary layer is not resolved adequately, the underlying physics of the flow is lost and the simulation will be erroneous. On the other hand, in the rest of the domain where the variations of temperature and velocity are small, the use of a fine mesh will lead to increases in the computation time without any significant improvement in accuracy. Thus, a nonuniform grid system is necessary to properly resolve the physics of the flow.

As shown in Fig. 1b – describing the dominium of a 660 cm^3 jar (H/D = 1.56) – a nonuniform grid system was used in the simulations. An unstructured mesh with 1,795 nodes and 3,394 triangular elements was developed, graded in both directions with a finer grid near the wall. To achieve this meshing, a maximum element size of 1.5 mm in the food boundary and an element growth rate of 1.25 were specified. This will give the adequate number of elements near the wall. The use of finer mesh showed no significant effect on the accuracy of the solution. The natural convection heating, for that jar, was simulated for 2,595 s. It took 100 steps to achieve the first 645 s, another 100 steps to reach 2,145 s and 230 steps for the total of 2,595 s of heating. Solutions have been obtained using a variety of grid sizes and time steps, and the results show that the solutions are time-step independent and weakly dependent on grid variation. Similar meshing and time steps were used for the different containers analyzed in this work.

Finally, the approximation of vessel geometry to a cylinder was validated. It was determined that the use of either domain

("exact" or "approximate") in the simulation model results in differences lower than 3.29% for cooking value and of 5.69% for lethality, without changes in the location of the SHZ.

Validation of the Model

Tests were performed in a laboratory scale still retort built in stainless steel, with a holding capacity of 27 or 12 containers of 360 or 660 cm^3 volumes, respectively. This retort is furnished with an automatic security valve that opens at the pressure of 2 atmospheres, reaching and maintaining a final temperature of approximately 118C. This type of retort and working temperature are typical to little-volume processors.

Temperatures within the retort, at the jar wall ($\xi = 1.00$) and at different positions ($\xi = 0.55$, $\zeta = 0.21$; $\xi = 0.55$, $\zeta = 0.47$; $\xi = 0.55$, $\zeta = 0.83$) within of a container of 660 cm^3 (H = 13.7) filled with CMC 0.85% w/w were measured, each 15 s, using Type T – copper-constantan – (Cu-CuNi) thermocouples of 0.5 mm thickness. The metallic lids of the containers were drilled in the center to let the passage of the thermocouples. A high-temperature resistant seal was used to secure air tightness around the thermocouple in the lid. Thermal histories were measured and recorded using a multi-channel data acquisition system (DASTC, Keithley, Cleveland, OH).

Both prediction methods were validated by comparing simulated temperatures against the experimental ones. To perform these comparisons, average absolute percent residues, as defined in Eq. (15), were used:

$$R = \frac{1}{m}\sum_{i=1}^{m}\frac{|T_{si} - T_e|}{T_e}100 \tag{15}$$

Determination of the Sterilization Times

Sterilization time was determined on the basis of the SHZ temperature. Then, the time it takes that point to reach an accumulated lethality (F_{100}^{15}) of 1.55 min was calculated as recommended for those products of high viscosity and acidity such as tomato sauce.

Accumulated lethalities were calculated in the usual way, by means of Eq. (16), as the integral of the lethal rate L along the processing time.

$$F = \int L dt = \int 10^{(T_c(t) - T_{ref})/z_e}\, dt \tag{16}$$

Cooking Value

The average cooking value (C_{ave}) was determined by numerical integration of Eq. (17), using the simulated temperature profiles for each sample. A reference temperature (T_{ref}) of 100C and a z_c value of 23C were considered for calculations. The value of z_c was chosen as the average of those values corresponding to the deterioration kinetics of sensory quality parameters (Ohlsson 1980).

$$C_{ave} = \int_0^{t_f}\left(\frac{\int_{\Omega_2} 10^{\frac{T(t,\Omega)-T_{ref}}{z_c}}\partial\Omega}{\int_{\Omega_2}\partial\Omega}\right)\partial t \tag{17}$$

RESULTS AND DISCUSSION

Flow Patterns and Temperature Profiles

Figure 2a–d shows predicted velocity vector and temperature profiles of viscous liquids for different glass containers after 3,000 s of heating. The lengths of the arrows represent magnitude of the velocities and the arrowheads represent the direction. When the liquid gets in contact with the wall, temperature rises leading to a density decrease. Due to this uneven distribution of density, buoyancy forces are produced and make the liquid move. The buoyancy force produces an upward flow near the wall. The rising hot liquid is deflected by the lid, and then it travels radially toward the center of the jar. Thus, a recirculating flow is created. Figure 2 also shows that the liquid adjacent to the wall and lid is at rest because of the no-slip boundary conditions. Figure 2 shows that axial velocities are higher for containers with a high height/diameter (H/D) ratio, than those with lower values of H/D. On the other hand, for the same sterilization time, bigger containers (660 cm^3, Fig. 2a,b) reach – as expected – lower temperatures than those of 360 cm^3 (Fig. 2c,d).

Figure 3 shows the experimental and predicted thermal histories at various points ($\xi = 0.55$, $\zeta = 0.21$; $\xi = 0.55$, $\zeta = 0.47$; $\xi = 0.55$, $\zeta = 0.83$) in the domain for a jar of 660 cm^3 (H = 13.7 cm) during thermal processing with variable external medium temperature.

Retort temperature shows two characteristic periods: the initial one which steadily increases up to approximately 80C, and then it reaches a less pronounced slope and the second one at constant temperature that is regulated by the internal pressure in the retort. On the other hand, temperatures measured in jar wall follow similar trend to that of the retort, lowering the difference between both with the advance of heating. Both temperatures level at about 1,500 s after the beginning of sterilization.

Simulated temperatures for different axial positions (ζ), and at the same radial position ($\xi = 0.55$) evidenced different delays which became greater near the bottom of the container. These differences could be due to the circulating flow as well as to the asymmetry of thermal conductivities between the bottom and the upper part of the jar (lid).

Predicted temperatures were found to be in satisfactory agreement with experimental measurements. Average abso-

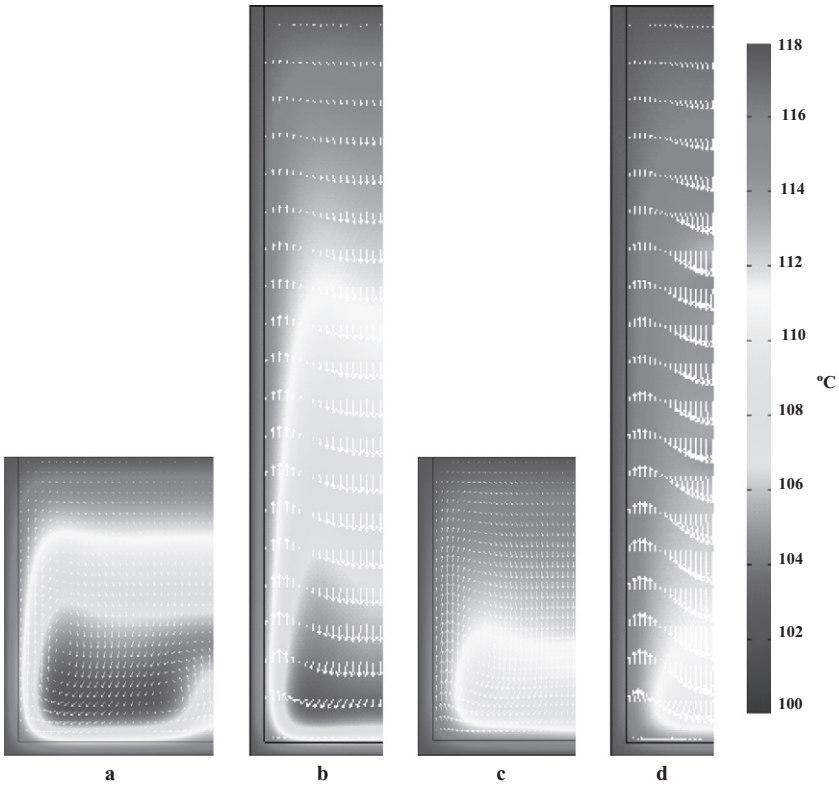

FIG. 2. VELOCITY VECTORS AND TEMPERATURE PROFILES, AT 3,000 S OF HEATING, FOR THE FOLLOWING CONTAINERS: V = 660 cm^3: (A) H = 8 cm AND D = 11.32 cm, (B) H = 20 cm AND D = 7.35 cm; V = 360 cm^3: (C) H = 8 cm AND D = 8.57 cm, (D) H = 20 cm AND D = 5.64 cm. THE RIGHT-HAND SIDE OF EACH FIGURE IS THE AXIS OF SYMMETRY

lute percent residues calculated according to Eq. (15), for the predicted temperatures, were lower than 4%, assessing the validity of the simulation model. All the numerical runs were tested for their computational speed, the maximum central processing unit time was 5.51 min using a personal computer (Intel, Santa Clara, CA) (R) Pentium (R) 4 with a processor speed of 3 GHz and a random access memory of 1.98 GB.

Figure 4 shows the change in axial velocities with time for a jar of 660 cm^3 (H = 16 cm). At the beginning, the magnitude of the velocity vectors increased with time, but as heating progressed, the velocity decreased. This variation of velocity can be explained in terms of the Grashof number, which represents the ratio of the buoyancy force to viscous force and its magnitude is indicative of laminar, transition and turbulent

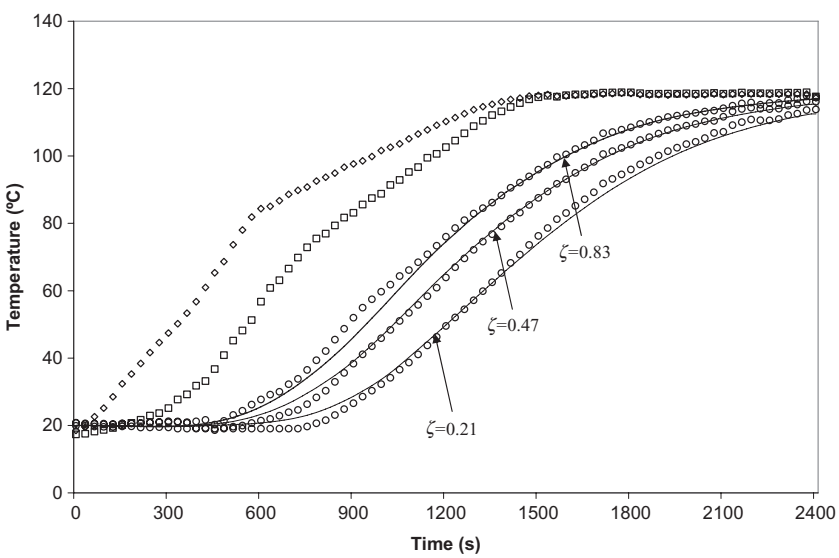

FIG. 3. EXPERIMENTAL (○) AND PREDICTED (CONTINUOUS LINES) TIME–TEMPERATURE CURVES FOR VARIOUS AXIAL POSITIONS AT SAME RADIAL POSITION (ξ = 0.55) FOR A JAR OF 660 cm^3 (H = 13.7 cm). RETORT TEMPERATURE (◇) AND WALL TEMPERATURE (□) ARE ALSO SHOWN

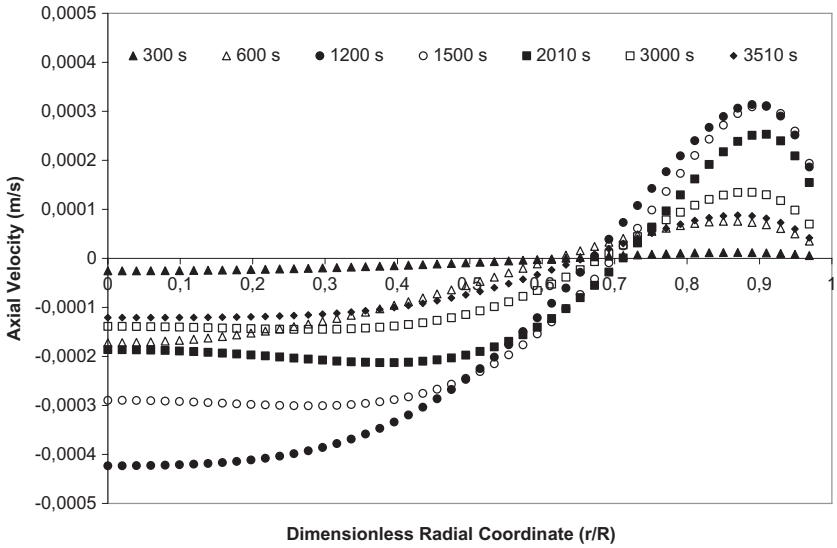

FIG. 4. AXIAL VELOCITY AT MID-HEIGHT ($\xi = 0.5$) VS. RADIAL POSITION FOR A JAR OF 660 cm^3 (H = 16 cm) AT DIFFERENT TIMES

flow regimes in natural convection. As heating progresses, a more uniform temperature is reached, reducing the buoyancy force in the liquid and leading to a significant reduction of velocity. Temperatures at all points tend to reach the temperature of the heating medium, and consequently the buoyancy forces disappear. The magnitude of Grashof number for the viscous liquid used in our simulation was in the range of 10^2–10^1 (using maximum temperature difference and minimum viscosity). The low Grashof numbers during the entire thermal treatment justify the laminar flow assumption.

The magnitude of the velocity vector was maximal at around 1,200 s of heating. The maximal axial velocity was found to be in the negative direction on the centerline of the jar. A similar behavior was always evidenced during the evolution of velocities with time, and their magnitudes were found to be in the order of 10^{-4} m/s; they were quite similar to those reported by Ghani *et al.* (1999a) for the same liquid, though under constant boundary conditions (121C).

Figure 4 also shows that the distance between the location of the stagnant region and the wall, named thickness of the ascending liquid, was about 30% of the radius (about 50% of the cross section of the jar). These values are lower than those determined by Ghani *et al.* (1999a) and Kumar *et al.* (1990), who reported values of 40 and 50%, respectively, for CMC. Differences are probably the result of a slower heating rate used in our system.

Figure 5 displays the maximal axial velocities developed for every container as a function of the *H/D* ratio, calculated after 1,500 s of heating (approximate moment when this maximum is reached for our heating regimes). It is evident

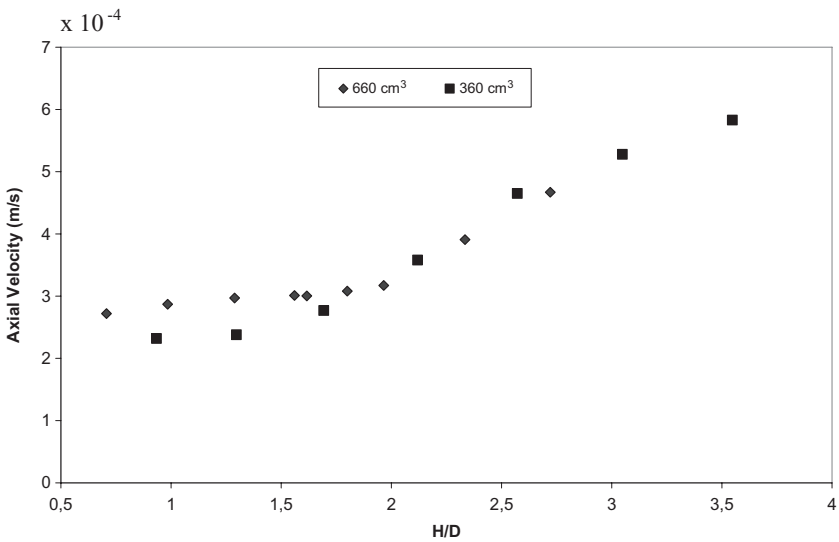

FIG. 5. MAXIMAL AXIAL VELOCITIES DEVELOPED AS A FUNCTION OF THE *H/D* RATIO, AT 1,500 S HEATING

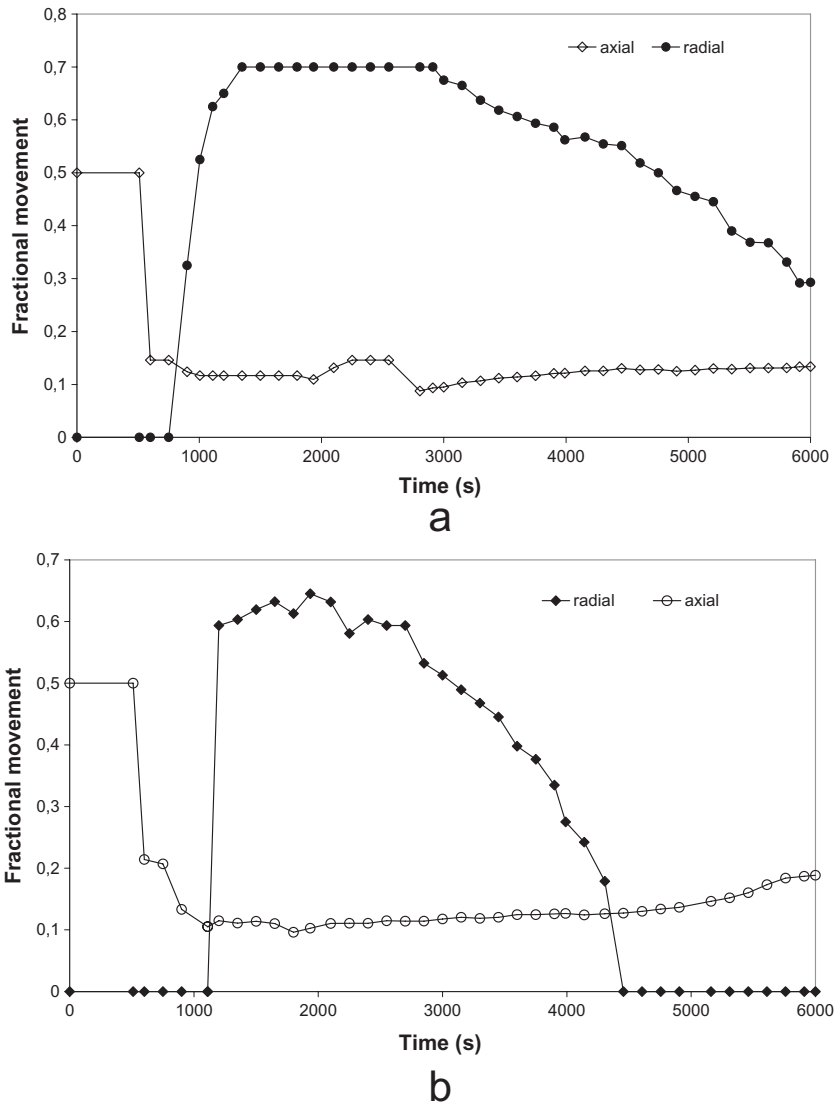

FIG. 6. FRACTIONAL MOVEMENT OF THE COLD POINT FOR: (A) JAR OF 660 cm^3 (H = 13.7 cm) AND (B) JAR OF 360 cm^3 (H = 12.0 cm)

that these velocities increase along with the *H/D* ratio for both volumes of containers studied. This result is in agreement with that shown in Fig. 2 where those jars with high *H/D* ratios (Fig. 2b,d) showed greater velocities.

SHZ Location

For the food processing engineer, the objective is to provide adequate thermal treatment, which will ensure that the SHZ receives the necessary heat for a sufficient period of time to inactivate the most damaging microorganisms, while maintaining sensory and nutritional properties. The location of the SHZ is influenced by the CP. The CP is defined as the location within a container of the product of the lowest temperature at a given time (Zechman and Plug 1989). Thus, the location of the CP is a critical parameter for the thermal process design. Tracking of the CP's axial and radial movements is shown in Fig. 6 for two glass containers of different volumes and dimensions. As shown in the figure, the location of the CP in the container moves during convection heating. The mode of heat transfer is initially conductive, and the position of the CP was found to be near the geometric center. Concerning jars, asymmetry exists between the thick glass bottom and the upper neck with its metal lid. A jar is an axisymmetric body, and then the CP will be located along the vertical axis of symmetry under the geometric center. As heating advances, the predominant transfer mode changes to convection and the CP moves from the geometric center toward the bottom of the jar. After a certain period of heating, the CP settles at a small bounded region for a relatively long period of time. This zone is known as slowest heating zone (SHZ).

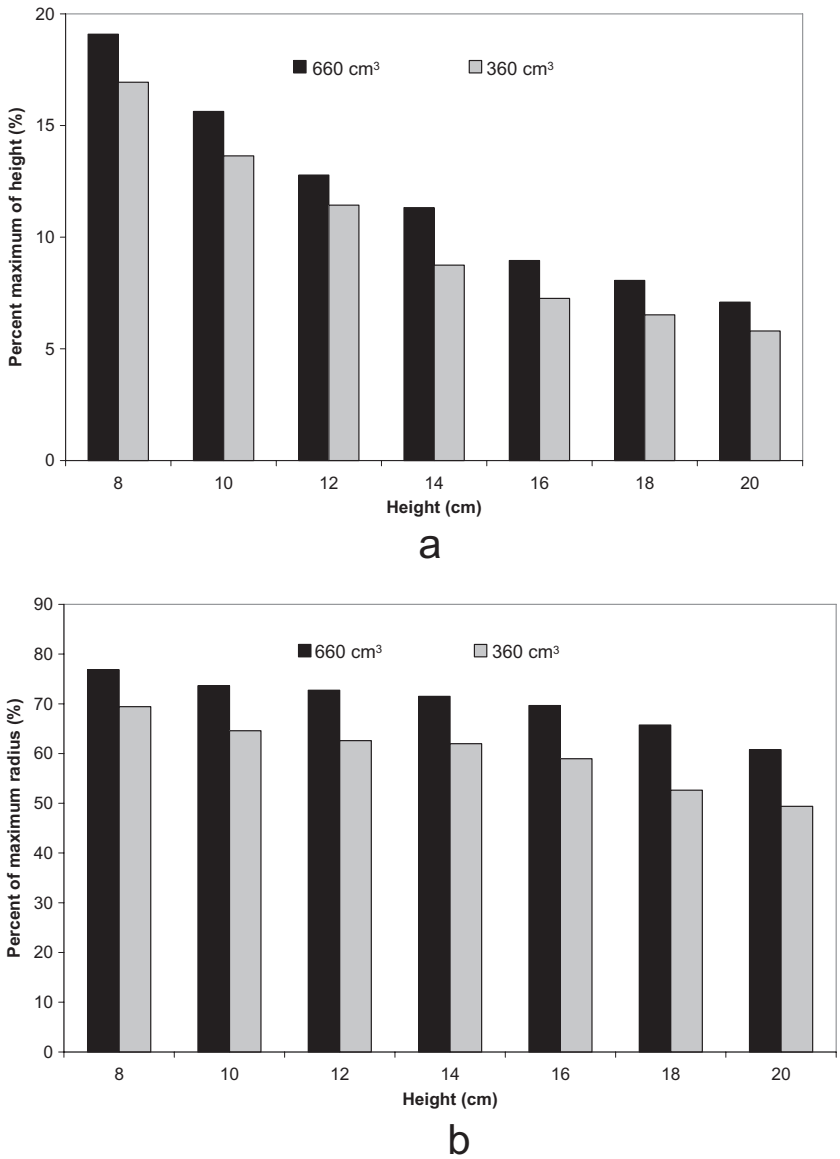

FIG. 7. POSITION OF SHZ FOR JARS OF DIFFERENT SIZES: (A) AXIAL POSITION EXPRESSED AS PERCENT OF MAXIMUM HEIGHT AND (B) RADIAL POSITION EXPRESSED AS PERCENT OF MAXIMUM RADIUS

Coordinates of position and time at which the CP is kept may vary according with the geometric aspect of the jar and its volume. In both cases, such a position is reached after 1,200 and 1,350 s in jars of 360 and 660 cm^3, respectively, whereby the jar of the greater size keeps the CP at the same position during longer periods of time and – as a consequence – the SHZ involves a lower volume. This difference may account for the fact that a smaller container is more rapidly heated, and hence the temperature profiles become uniform sooner. Due to this temperature uniformity, the natural convection flow diminishes and conduction, indeed, becomes the main mode of heat transfer. Then, the CP starts moving in the reverse direction. This movement is an indication of the change of mode of heat transfer from convective to conductive. In this work, the simulation time was restricted to 6,000 s, then the CP could not reach its original position.

Localization of the SHZ – defined as the average coordinates of successive coldest points that are involved in it – is expressed as height and radius percentage, for the different containers analyzed. It is displayed in Fig. 7a,b, respectively, for the different containers analyzed. The values obtained were in the range of 5.81–19.09% of the jar height, and 49.53–76.83% of the jar radius, depending on the volume and geometric aspect. These observations are in agreement with those reported by Kumar and Bhattacharya (1991), Datta and Teixeira (1988), Zechman and Plug (1989), Ghani *et al.* (1999a), who reported values from 10 to 15% height from the bottom of the can (with a radius of 0.0405 m and height of 0.111 m).

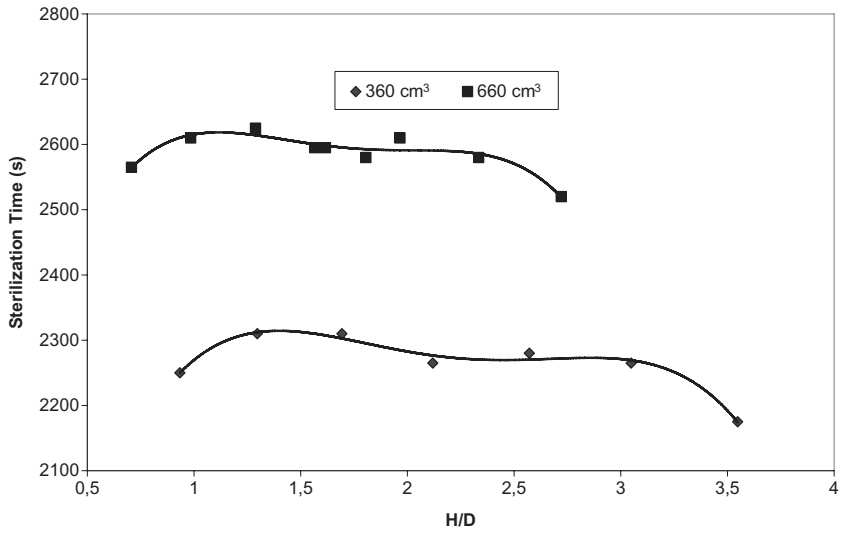

FIG. 8. STERILIZATION TIMES FOR VARIOUS CONTAINERS AS A FUNCTION OF *H/D*

Effect of Geometry Aspect on the Sterilization Times

Figure 8 shows the sterilization times that were estimated as a function of the *H/D* ratio corresponding to each jar. Thus, for 660 cm^3 containers, sterilization time ranged from 2,520 to 2,625 s. As expected, 360 cm^3 containers showed shorter sterilization times (2,175–2,310 s) than those of 660 cm^3. Both volumes of containers evidenced a similar behavior concerning variation of sterilization time with *H/D* ratio, showing a slight decrease in both ends of the *H/D* ratio. For these sterilization times, temperatures reached in the SHZ were similar for equal volume jars, being of approximately 96 and 94C for jars of 360 and 660 cm^3, respectively. This parameter (final temperature) could be chosen, instead of accumulated lethality, as a simple way for the estimation of sterilization time.

With the aim of estimating sterilization times, in the function of container volume and geometric aspect, a polynomial regression was obtained from predicted data, with the following structure:

$$t_{process} = a\,(H/D)^4 + b\,(H/D)^3 + c\,(H/D)^2 + d\,(H/D) + e \quad (18)$$

Table 3 presents the values of parameters *a*, *b*, *c*, *d* and *e* and the correlation coefficients (R^2) for the two container volumes studied.

Based on this equation, it is possible to estimate process times for vessels with any *H/D* ratio in the range studied in this work (0.7–2.72 and 0.97–4.05 for jars of 660 and 360 cm^3, respectively).

Cooking Value

Simulated average cooking values (C_{ave}), calculated for the sterilization times previously estimated for each jar, are shown in Fig. 9. It can be observed in this figure that the lower cooking value is obtained – for both sizes – for the lower jar height (8 cm) and higher jar diameter. For both sizes, the higher cooking value was predicted for containers with a height of 18 cm. All this information shows that the modification of container size and/or shape induces changes in the final quality of the processed food.

CONCLUSIONS

Profiles of temperature and velocity were simulated using the method of finite elements during heating of a viscous liquid food (CMC), packed in glass containers of different volumes and sizes. Based on this, the SHZ movement was determined, and its location was found to be unaltered for a certain period of time. Also, sterilization times were calculated in order to reach the point of microbial inactivation. The geometric aspect of the container was found to have considerable effect on the localization of the SHZ, values of temperatures and velocity profiles and – as a consequence – on process times. For this last parameter, differences of up to 135 and 105 s for jars

Volume (cm^3)	*a*	*b*	*c*	*d*	*e*	R^2
360	–61.55	550.64	–1,777.30	2,413.90	1,144.00	0.9756
660	–112.90	780.50	–1,961.00	2,088.70	1,820.20	0.9056

TABLE 3. PARAMETERS OF THE REGRESSION MODEL AND CORRELATION COEFFICIENTS

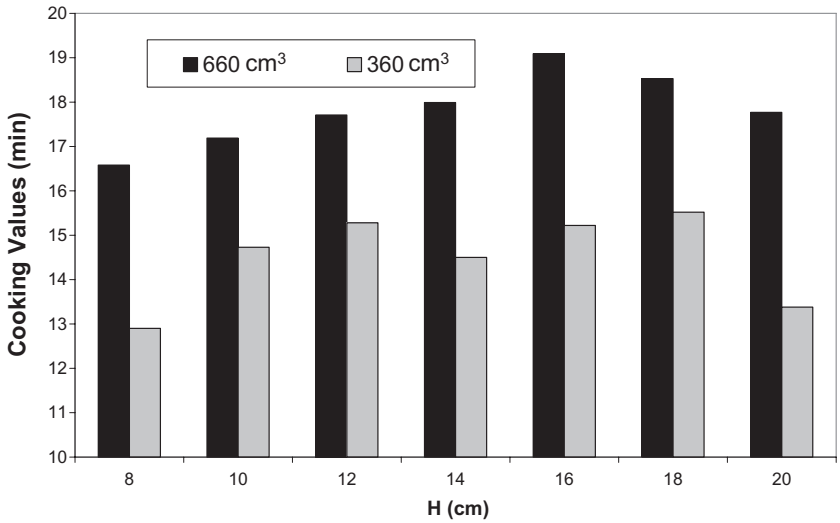

FIG. 9. COOKING VALUES FOR CONTAINERS OF DIFFERENT SIZES

of 360 and 660 cm^3, respectively, were found. As a consequence, cooking values showed variations for the different jar sizes, these been lower for those containers with lower height.

When a container is replaced for another of the same volume but different H/D ratio, the needed sterilization time varies; therefore, it is not accurate to use the same sterilization time for all the containers of the same size, irrespective of their aspect ratio. In this sense, a prediction method was developed for the calculation of sterilization times in a simple and accurate way as a function of size and shape. This method can be useful for process design for low-volume productions, where sterilization is discontinuous and is usual to work with successive batches of jars of different sizes and shapes. These industries normally lack of adequate numerical calculation softwares for process design.

NOMENCLATURE

C_p	specific heat (J/kg/K)
CP	cold point
CMC	carboxy-methyl cellulose
D	diameter of jar (m)
Gr	Grashof number, $Gr = g\beta\Delta TH^3\rho^2/\mu^2$
g	acceleration due to gravity (m/s^2)
H	height of the jar (m)
k	thermal conductivity (W/m/K)
L	lethal rate
m	number of experiment temperatures compared
P	pressure (Pa)
R	radius of the jar (m)
r	radial position respect of centerline (m)
SHZ	slowest heating zone
t	time (s)
T	temperature (°C or K)
u	velocity in vertical direction (m/s^1)
V	volume (cm^3)
z	distance in vertical direction from the bottom (m)
z_c	thermal resistance factor (°C)

Greek Symbols

ρ	density (kg/m^3)
Ω	domain
Ω_1	solid phase domain
Ω_2	liquid phase domain
$\partial\Omega_1$	glass jar boundary
$\partial\Omega_2$	solid-liquid interface
$\partial\Omega_3$	symmetry axis
ν	velocity in radial direction (m/s^1)
ζ	dimensionless height (z/H)
ξ	dimensionless radial position (r/R_{ext})
β	thermal expansion coefficient (K^{-1})
μ	apparent viscosity (Pa s)

Subscripts

c	thermal center of the heating product
e	experimental
ext	external
i	initial
int	internal
l	liquid phase
ref	reference
s	solid phase
si	simulated
w	wall
Wt	wall thickness

ACKNOWLEDGMENTS

Authors acknowledge the financial support of CONICET, UNLP and ANPCyT from Argentina.

REFERENCES

ADRIAN, B. 1993. *Heat Transfer*, Wiley, New York, NY.

BIRD, R.B., STEWART, W.Y. and LIGHTFOOT, E.N. 1976. *Transport Phenomena*, John Wiley and Sons, New York, NY.

COMSOL, A.B. 2005. COMSOL Multiphysics User's Guide. Version: September 2005, COMSOL 3.2.

DATTA, A.K. and TEIXEIRA, A.A. 1988. Numerically predicted transient temperature and velocity profiles during natural convection heating of canned liquid foods. J. Food Sci. *53*, 191–195.

GHANI, A.G., FARID, M.M. and CHEN, X.D. 2002. Numerical simulation of transient temperature and velocity profiles in a horizontal can during sterilization using computational liquid dynamics. J. Food Eng. *51*, 77–83.

GHANI, A.G., FARID, M.M., CHEN, X.D. and RICHARDS, P. 1999a. Numerical simulation of natural convection heating of canned food by computational fluid dynamics. J. Food Eng. *41*, 55–64.

GHANI, A.G., FARID, M.M., CHEN, X.D. and RICHARDS, P. 1999b. An investigation of deactivation of bacteria in a canned food during sterilization using computational liquid dynamic. J. Food Eng. *42*, 207–214.

GHANI, A.G., FARID, M.M. and ZARROUK, S.J. 2003. The effect of can rotation on sterilization of liquid food using computational liquid dynamics. J. Food Eng. *57*, 9–16.

KIZILTAS, S., ERDOGDU, F. and PALAZOGLU, T.K. 2010. Simulation of heat transfer for solid-liquid food mixtures in cans and model validation under pasteurization conditions. J. Food Eng. *97*, 449–456.

KUMAR, A. and BHATTACHARYA, M. 1991. Transient temperature and velocity profiles in a canned non-Newtonian food during sterilization in still-cook retort. Int. J. Heat Mass Transf. *34*, 1083–1096.

KUMAR, A., BHATTACHARYA, M. and BLAYLOCK, J. 1990. Numerical simulation of natural convection heating of canned thick viscous liquid food products. J. Food Sci. *55*, 1403–1411.

MARRA, F. and ROMANO, V. 2003. A mathematical model to study the influence of wireless temperature sensor during assessment of canned food sterilization. J. Food Eng. *59*, 245–252.

NAVEH, D., KOPELMAN, I.J. and PFLUG, I.J. 1983. The finite element method in the thermal processing of foods. J. Food Sci. *48*, 1086–1093.

OHLSSON, T. 1980. Temperature dependence of sensory quality changes during thermal processing. J. Food Sci. *45*, 836–847.

PORNCHALOEMPONG, P., BALABAN, M.O., TEIXEIRA, A.A. and CHAU, K.V. 2003a. Numerical simulation of conduction heating in conically shaped bodies. J. Food Process Eng. *25*, 539–555.

RABIEY, L., FLICK, D. and DUQUENOY, A. 2007. 3D simulations of heat transfer and liquid flow during sterilization of large particles in a cylindrical vertical can. J. Food Eng. *82*, 409–417.

STEFFE, J.F., MOHAMED, I.O. and FORD, E. 1986. Rheological properties of fluid foods. Data compilation. In *Physical and Chemical Properties of Foods* (M.R. Okos, ed.) ASAE, St. Joseph, MO.

VARMA, M.N. and KANNAN, A. 2005. Enhanced food sterilization through inclination of the container walls and geometry modifications. Int. J. Heat Mass Transf. *48*, 3753–3762.

VARMA, M.N. and KANNAN, A. 2006. CFD studies on natural convective heating of canned food in conical and cylindrical containers. J. Food Eng. *77*, 1024–1036.

WELTI CHANES, J., GÓMEZ PALOMARES, O., VERGARA BALDERAS, F. and ALZAMORA, S.M. 2005. Aplicaciones de ingeniería y fenómenos de transporte al estudio de la transferencia convectiva de calor en alimentos envasados. Revista Mexicana Ingeniería Química *4*, 89–106.

ZECHMAN, L.G. and PLUG, I.J. 1989. Location of the slowest heating zone for natural convection heating fluids in metal containers. J. Food Sci. *54*, 205–229.